Unified model of ultracold molecular collisions

James F. E. Croft, John L. Bohn, Goulven Quéméner

A unified model of ultracold molecular collisions

James F. E. Croft
The Dodd-Walls Centre for Photonic and Quantum Technologies, New Zealand and Department of Physics, University of Otago, Dunedin, New Zealand

John L. Bohn
JILA, NIST, and Department of Physics, University of Colorado, Boulder, Colorado 80309-0440, USA

Goulven Quéméner
Université Paris-Saclay, CNRS, Laboratoire Aimé Cotton, 91405, Orsay, France

A scattering model is developed for ultracold molecular collisions, which allows inelastic processes, chemical reactions, and complex formation to be treated in a unified way. All these scattering processes and various combinations of them are possible in ultracold molecular gases, and as such this model will allow the rigorous parametrization of experimental results. In addition we show how, once extracted, these parameters can to be related to the physical properties of the system, shedding light on fundamental aspects of molecular collision dynamics.

I. INTRODUCTION

Ultracold samples of molecules can be exquisitely controlled at the quantum state level, allowing fundamental physical and chemical process to be studied with unprecedented precision. This control has been used to study state-to-state chemistry with full quantum state resolution for all reactants and products [1], to probe the potential energy surface with exquisite resolution [2, 3], and to study the role of nuclear spins in molecular collisions [4, 5], More recently an experiment has managed to probe the intermediate complex of an ultracold ultracold reaction [6] as such it is now possible to track the complete chemical process from reactants, through intermediates, to products.

Understanding the fundamental physical and chemical process of ultracold molecular collisions is also important because ultracold gases are fragile systems, prone to collisional processes that can transfer their atomic or molecular constituents into untrapped states or else release large amounts of kinetic energy, leading to trap loss and heating. A new mechanism for loss in an ultracold molecular gas was proposed [7, 8], namely a half-collision process in which the reactant molecules share energy in rotational and vibrational degrees of freedom, spending a long time lost in resonant states of a four-body collision complex rather than promptly completing the collision process. This idea of transient complex formation, colloquially dubbed "sticking", takes on an added significance for ultracold molecular collisions where the number of available exit channels can be very small compared to the number of resonant states.

Initial experiments on non-reactive ultracold molecules, such as NaRb [9, 10] and RbCs [11], observed two-body collisional losses, even though these species are non-reactive and are in their quantum mechanical ground state, so have no available inelastic loss channels. As these complexes were not directly observed, it remained an open question whether these experiments have produced long-lived collisional complexes and what the loss mechanism was. However, a subsequent experiment on RbCs [12] showed that turning on or off the trapping light that confines the molecules can increase or decrease the losses of the molecules. This confirmed the hypothesis of a theoretical study [13] that the non-reactive molecules first form tetramer complexes, and then the complexes are lost due to light scattering in the optical dipole trap. In addition, an experiment on chemically reactive ultracold molecules such as KRb succeeded in directly observing the corresponding ions of the intermediate complex K_2Rb_2 [6], as well as of the products K_2 and Rb_2 of the chemical reaction. Just as for non-reactive molecules, the trapping light has a strong effect on the losses of the reactive molecules as well as on the lifetime of the transient complex [14], sharing the same conclusion as [12, 13]. It is therefore clear that any theoretical treatment of ultracold molecular collisions must be flexible enough to account for the formation of the complexes.

These experiments can be described by a model that assumes an absorption probability $p_{\rm abs}$ for any two molecules that get within a certain radius [15], without ascribing any particular mechanism to the absorption. Energy and electric field dependence of two-body loss rates are well-fit by the resulting formulas. For example, the reactive molecules in the KRb experiment vanish with unit probability $p_{\rm abs} = 1$ with or without electric field [4, 16, 17]. The non-reactive species NaRb and RbCs vanish with probabilities 0.89 [18] and 0.66 [11] respectively, in zero electric field. Notably, when an electric field is applied to NaRb, its absorption probability climbs to $p_{\rm abs} = 1$ [10]. Assuming the origin of this loss is due to complex formation, the increased loss with electric field may be attributed to the increased density of accessible states of the complex and/or coupling of these states to the continuum scattering channels. It is therefore conceivable that complex formation may be a phenomenon that can be turned on or off as desired.

While the influence of light scattering on molecular

collisions is undeniable, it should also be possible for the molecules to be confined in "box" traps, where the molecules remain mostly in the dark, encountering trapping light only at the peripheries of the trap [19]. In this case, loss due to complex formation would allow a more direct probe of the fundamental four-body physics of the collision.

In this paper we propose a phenomenological model of collisional losses, based on the theory of average cross sections [20], that encompasses both direct collisional losses and loss due to complex formation. As such this model serves not only to parametrize experimental measurements, but also allows those parameters to be related to the physical properties of the system, potentially shedding light on the dynamics of the molecular complex.

II. THEORY

The theory must be flexible enough to describe the various outcomes available when two molecules collide. These include elastic scattering of the reactants; inelastic scattering, where the reactants emerge with the same chemical identity but in different internal states; reactive scattering into various product states; and absorption into the collision complex. Moreover, depending on the experiment, the various outcomes of the collision may or may not be observed. Note that, within this model, formation of a collision complex will always be regarded an outcome in and of itself: we do not consider where the complex ultimately decays to.

A. Molecular scattering, observed and unobserved processes

To this end, we define a flexible system of notation as illustrated in Fig. 1. This figure shows schematically the distance r between two collision partners (which may be reactants or products), and the various possible outcome channels. Channels whose outcome is observed by a particular experiment are labelled by roman letters while channels whose outcome is unobserved are labelled by greek letters. The channels labelling observed processes are further differentiated as follows. Channels labelled a, b, c, ... correspond to the *elastic* and *inelastic* channels of the reactants, while channels labelled k, l, m, ... correspond instead to channels of a different molecular arrangement and correspond to the product channels of a *chemical reaction*. Note that the unobserved processes may include both inelastic scattering, as well as chemical reactions: the criterion is simply that this outcome is not observed.

By convention, we take a to label the incident channel. In general, scattering events that initiate in channel a and terminate in any channel i, where i serves as a running index, are described by the elements S_{ia} of a scattering matrix $\boldsymbol{S}$. The list of channels i will of course depend on the details of a particular experiment. In some experiments, all the final states can be measured so that there are no channels denoted by greek letters, while in others none of the final states can be measured so that there are no channels denoted by roman letters (except the incident channel a). In some experiments, inelastic channels are measured but reactive ones are not, or vice versa. Therefore one has to determine which processes are labelled as observed or unobserved processes for a particular experiment of interest. In Sec. II D, we will detail how these unobserved processes can be gathered into an overall, absorption term.

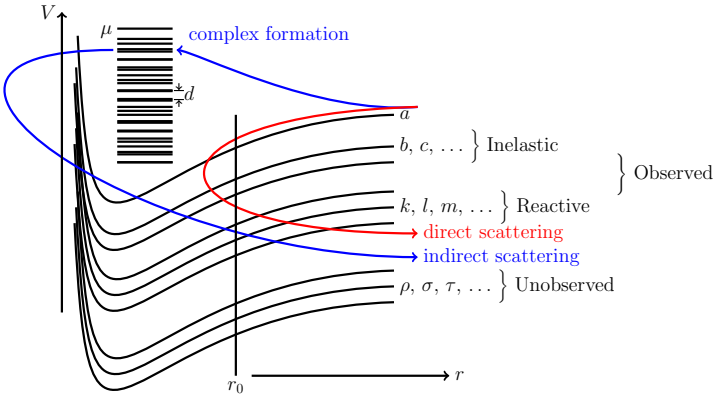

FIG. 1. Schematic outlining the various scattering processes and channel labels. Direct and indirect scattering processes are shown by red and blue arrows respectively. The incoming channel is labelled a; inelastic scattering channels that can be observed in an experiment are denoted by roman letters b, c, ...; reactive scattering channels that can be observed in an experiment are denoted by roman letters k, l, m, ...; inelastic or reactive channels that are unobserved in a given experiment are denoted by letters ρ, σ, τ, ... Finally a dense forest of resonant states labelled by μ of the collision complex, of, with a mean level spacing d, is shown in the well of the potential.

The observed and unobserved processes are those that are expected to produce inelastic scattering or chemical reactions immediately, that is, without forming a collision complex, shown in Fig. 1 by the red arrow labelled *direct scattering*. Typically, the results of these processes release kinetic energy greater than the depth of the trap holding the molecules, and hence lead to what we term *direct loss*. By contrast, *indirect scattering* processes which proceed via *complex formation*, shown in Fig. 1 by the blue arrows, will not immediately lead to trap loss. Molecules lost into the collision complex require a second step to leave the trap, which consists of either absorbing a photon of trapping light, colliding with another molecule, or decaying into an allowed channel of reactants or products. The present theory will not explicitly address this second step, focusing only on the formation of the complex.

B. Scattering cross sections for various processes

Corresponding to each S-matrix element is the state-to-state probability of a scattering process from channel a to channel i, with $i = a, b, c, \ldots, k, l, m, \ldots, \rho, \sigma, \tau, \ldots$, given by

$$p_{a\to i} = |S_{ia}|^2. \tag{1}$$

As the S-matrix is unitary, we have for each incident channel a

$$\begin{aligned} 1 &= \sum_{\substack{i=a,b,c,\ldots,\\ k,l,m,\ldots}} |S_{ia}|^2 + \sum_{i=\rho,\sigma,\tau,\ldots} |S_{ia}|^2 \\ &\equiv p_{\rm obs} + p_{\rm unobs}, \end{aligned} \tag{2}$$

where we have separated the scattering matrix into an observed block (i running on roman letters) and unobserved block (i running on greek letters).

The probability for observed processes, $p_{\rm obs}$, can be further subdivided into elastic, inelastic and reactive parts $p_{\rm obs} = p_{\rm el} + p_{\rm in} + p_{\rm re}$, with

$$\begin{aligned} p_{\rm el} &= p_{a\to a} = |S_{aa}|^2 \\ p_{\rm in} &= \sum_{i=b,c,\ldots} p_{a\to i} = \sum_{i=b,c,\ldots} |S_{ia}|^2 \\ p_{\rm re} &= \sum_{i=k,l,m,\ldots} p_{a\to i} = \sum_{i=k,l,m,\ldots} |S_{ia}|^2. \end{aligned} \tag{3}$$

There is of course no reason to subdivide unobserved processes in this way.

In general, if some processes are unobserved, then from Eq. (2), the observed block of the scattering matrix will appear sub-unitary:

$$\sum_{i=a,b,c,\ldots,k,l,m,\ldots} |S_{ia}|^2 \le 1. \tag{4}$$

The amount by which this sum falls short of unity will be a measure of the unobserved probability, which in general is recast into an overall, absorption probability $p_{\rm abs}$. Therefore

$$p_{\rm abs} \equiv p_{\rm unobs} = 1 - p_{\rm obs} = 1 - p_{\rm el} - p_{\rm in} - p_{\rm re}. \tag{5}$$

In the next subsection we will see that collisions resulting in complex formation can also be properly included in the absorption probability. It is also convenient to define a quenching probability, which is the sum of the inelastic, reactive and absorption probabilities

$$p_{\rm qu} = p_{\rm in} + p_{\rm re} + p_{\rm abs} = 1 - p_{\rm el} = 1 - |S_{aa}|^2. \tag{6}$$

Finally, the corresponding state-to-state cross section is given by

$$\sigma_{a\to i} = g\frac{\pi}{k^2}|\delta_{ai} - S_{ia}|^2, \tag{7}$$

where $g = 2$ if the identical collision partners are initially in the same quantum mechanical state, and $g = 1$ otherwise. The cross sections corresponding to these processes are given by

$$\begin{aligned} \sigma_{\rm el} &= g\frac{\pi}{k^2}|1 - S_{aa}|^2, \\ \sigma_{\rm in} &= g\frac{\pi}{k^2}\ p_{\rm in}, \\ \sigma_{\rm re} &= g\frac{\pi}{k^2}\ p_{\rm re}, \\ \sigma_{\rm abs} &= g\frac{\pi}{k^2}\ p_{\rm abs}, \\ \sigma_{\rm qu} &= \sigma_{\rm in} + \sigma_{\rm re} + \sigma_{\rm abs}. \end{aligned} \tag{8}$$

C. Complex formation and highly resonant collisions

The treatment so far has ignored the possibility of complex formation. The collision complex is comprised of a dense forest of resonant states, depicted schematically in Fig. 1 by horizontal lines. These states, denoted μ, are potentially numerous and complicated, and are therefore best characterized by statistical quantities, such as their mean level spacing d (equivalently mean density of states $\rho = 1/d$) and their coupling matrix elements $W_{i\mu}$ to the open channels. For the purposes of a theory on complex formation, it is assumed that the lifetime of the complex is long compared to the mean collision time, so that the complex formation and decay are distinct events. This assumption appears to be validated by the observation of K_2Rb_2 complexes in KRb + KRb ultracold reactions [6] and by the measure of their lifetimes [14]. In this case, losses due to complex formation can also occur.

This process will be considered as an unobserved process, as defined in the previous section. We will see that the theory of highly resonant collisions can recast this type of loss into a phenomenological absorption term, included in the definition (5) as for the unobserved processes discussed above. This will also enter as a parameter of our theory in the following.

The key concept for understanding highly resonant collisions and the corresponding complex formation can be found in the compound nucleus (CN) model introduced by Bohr for understanding nuclear collisions [21]. This theory postulates that a compound state involving all the nucleons forms immediately when a particle (such as a neutron) encounters the nucleus. These compound states have long lifetimes which leads to a dense set of narrow resonances in the cross section as a function of energy. Since Bohr's initial insight, the statistical theory of highly resonant scattering has been developed considerably [20, 22–27]. We draw heavily on this literature in what follows.

The essential simplification of the statistical theory is the assumption that the density of states is too great for any of the individual resonances to be resolved, therefore scattering observables can be replaced by suitable averages [20, 24]. The virtue of this approach can be

illustrated using an example with a single channel, where the cross sections for elastic and absorption scattering are given by

$$\sigma_{\rm el} = g\frac{\pi}{k^2}|1-S|^2 \qquad \sigma_{\rm abs} = g\frac{\pi}{k^2}(1-|S|^2), \tag{9}$$

the overall absorption process accounting for all but the elastic process, similar to what can be seen in Eq. (8) and Eq. (5). If all the incident flux were reflected, then $|S|^2 = 1$ and there would be no absorption. If only a part of the flux were reflected $|S|^2$ would be less than unity, due to absorption. For indirect processes like complex formation, there is no true absorption: eventually the molecules re-emerge and complete a scattering event. However, long-lived complexes can give the appearance of absorption if the lifetime of the complexes is long enough, and moreover leads to true loss if the complex is destroyed by a photon or by a collision with another molecule. These effects are accounted for in the following. The lifetime and subsequent decay of the complex is not treated within the model we detail here.

In the statistical theory of scattering, the average of any energy-dependent quantity $f(E)$ can be defined as

$$\langle f(E)\rangle = \frac{1}{Z}\int d\epsilon\, f(\epsilon)\, D(E;\epsilon), \tag{10}$$

where $D(E;\epsilon)$ is the distribution, centered at E, that defines the average, and $Z = \int d\epsilon\, D(E;\epsilon)$. D is often taken to be either a Lorentzian function or else a finite step function centered at E. In any event, here D is assumed to be broad enough to contain many resonances. In these terms and factoring out the explicit momentum dependence, an average cross section can be written [24]

$$\langle\sigma\rangle = g\frac{\pi}{k^2}\,\langle k^2\sigma\rangle\,. \tag{11}$$

To calculate the average elastic cross section then requires taking the average $\langle|1-S|^2\rangle$. Using the definition for the variance for a variable X

$$\Delta X \equiv \langle|X|^2\rangle - |\langle X\rangle|^2, \tag{12}$$

we obtain

$$\langle|1-S|^2\rangle = |1-\langle S\rangle|^2 + \Delta S. \tag{13}$$

The average elastic cross section can therefore be written in the form

$$\begin{aligned}\langle\sigma_{\rm el}\rangle &= g\frac{\pi}{k^2}\,\langle|1-S|^2\rangle \\ &= g\frac{\pi}{k^2}|1-\langle S\rangle|^2 + g\frac{\pi}{k^2}\,\Delta S \\ &\equiv \sigma_{\rm se} + \sigma_{\rm ce}.\end{aligned} \tag{14}$$

These two contributions comprise a mean cross section, denoted the "shape elastic" cross section; and a contribution from the fluctuations, denoted the "compound elastic" cross section [20, 24]. Since the lifetime of a collisional process is proportional to the energy derivative of the S-matrix [28–31], writing the cross section in this way elegantly separates out the cross section for direct scattering, the shape elastic part, from indirect scattering, the compound elastic part. Meanwhile, the average absorption cross section is

$$\langle\sigma_{\rm abs}\rangle = g\frac{\pi}{k^2}(1-\langle|S|^2\rangle). \tag{15}$$

The essence of the CN model is to associate elastic scattering with just the shape elastic part of the elastic cross section and include the compound elastic part in the absorption cross section. This is achieved by simply making the replacement $S \to \langle S\rangle$ in Eq. (9). The elastic cross section in the CN model is therefore

$$\tilde{\sigma}_{\rm el} = g\frac{\pi}{k^2}|1-\langle S\rangle|^2 = \sigma_{\rm se}. \tag{16}$$

while the absorption cross section is

$$\begin{aligned}\tilde{\sigma}_{\rm abs} &= g\frac{\pi}{k^2}(1-|\langle S\rangle|^2), \\ &= g\frac{\pi}{k^2}(1-\langle|S|^2\rangle) + g\frac{\pi}{k^2}\,\Delta S \\ &= \langle\sigma_{\rm abs}\rangle + \sigma_{\rm ce}.\end{aligned} \tag{17}$$

again using the definition of the variance. As desired, simply by replacing S in Eq. (9) with $\langle S\rangle$, the compound elastic part now appears in the absorption cross section.

D. Generalized theory of average cross sections

Generalizing the averaging procedure above to the multichannel case, one incorporates the effect of resonant complex formation by energy averaging the appropriate cross sections over many resonances [32],

$$\begin{aligned}\langle\sigma_{a\to i}\rangle &= g\frac{\pi}{k^2}\,\langle|S_{ia}|^2\rangle \\ &= g\frac{\pi}{k^2}|\langle S_{ia}\rangle|^2 + g\frac{\pi}{k^2}\Delta S_{ia} \\ &\equiv \sigma^{\rm dir}_{a\to i} + \sigma^{\rm ind}_{a\to i}.\end{aligned} \tag{18}$$

Doing so defines two components of the scattering. The first component, associated with an energy-smooth S-matrix $\langle\boldsymbol{S}\rangle$, is *direct scattering* which is scattering from channel a to i which proceeds without forming a collision complex—this is the generalization of the "shape elastic" cross section in the single channel example above. The second component, associated with the energy fluctuations of the S-matrix ΔS, is *indirect scattering* which is also scattering from channel a to i but which proceeds via a collision complex—this is the generalization of the "compound elastic" cross section in the single channel example above.

Following the prescription of the CN model, the cross sections for any process whose outcome is observed are associated with the corresponding direct scattering cross

section. The elastic, inelastic, and reactive cross sections are therefore given by

$$\begin{aligned}\tilde{\sigma}_{\rm el} &\equiv \sigma_{\rm el}^{\rm dir} = g\frac{\pi}{k^2}|1-\langle S_{aa}\rangle|^2 \\ \tilde{\sigma}_{\rm in} &\equiv \sigma_{\rm in}^{\rm dir} = g\frac{\pi}{k^2}\sum_{i=b,c,\ldots}|\langle S_{ia}\rangle|^2 \\ \tilde{\sigma}_{\rm re} &\equiv \sigma_{\rm re}^{\rm dir} = g\frac{\pi}{k^2}\sum_{i=k,l,m,\ldots}|\langle S_{ia}\rangle|^2. \end{aligned} \tag{19}$$

These are presented as total cross sections, for example, $\tilde{\sigma}_{\rm in}$ is the total inelastic cross section and includes all inelastic scattering of molecules that is observed. If individual inelastic channels are resolved experimentally, they correspond to individual terms of this sum; and the same for reactive scattering.

Direct processes to channels that are not observed contribute to the absorption cross section, $\tilde{\sigma}_{\rm abs}$, and their total contribution is formally given by

$$\tilde{\sigma}_{\rm abs}^{\rm dir} \equiv \sigma_{\rm abs}^{\rm dir} = g\frac{\pi}{k^2}\sum_{i=\rho,\sigma,\tau,\ldots}|\langle S_{ia}\rangle|^2. \tag{20}$$

The cross section for complex formation also contributes to the absorption cross section, and is simply the total cross section for all indirect processes. As such it is given by

$$\begin{aligned}\tilde{\sigma}_{\rm abs}^{\rm ind} &\equiv \sigma_{\rm el}^{\rm ind} + \sigma_{\rm in}^{\rm ind} + \sigma_{\rm re}^{\rm ind} + \sigma_{\rm abs}^{\rm ind} \\ &= g\frac{\pi}{k^2}\sum_{\substack{i=a,b,c,\ldots,\\ k,l,m,\ldots,\\ \rho,\sigma,\tau,\ldots}}\Delta S_{ia}. \end{aligned} \tag{21}$$

The total absorption cross section is then the sum of the direct and the indirect contributions

$$\tilde{\sigma}_{\rm abs} = \tilde{\sigma}_{\rm abs}^{\rm dir} + \tilde{\sigma}_{\rm abs}^{\rm ind}. \tag{22}$$

This is the generalization of Eq. (17). In this theory, the matrix elements of the highly-resonant S-matrix S_{ia} (and therefore also ΔS_{ia}) are presumed to be unknown. Information about absorptive scattering will be inferred from the sub-unitarity of the energy averaged S-matrix, $\langle \boldsymbol{S}\rangle$, in the observed channels. Appropriate forms of these effective S-matrices will be derived in Sec. II F.

It should be emphasized that by treating the complex as an absorption process, we are describing only the phenomenon of molecules combining to form a collision complex. Eventually such a complex would decay producing outcomes in any available channel, but a full treatment of this process would require detailed understanding of the decay mechanism of the complex, or equivalently the full S-matrix on a fine enough energy grid that the appropriate averages given in Eqn. (18) could be meaningfully performed.

Finally, it is often useful to define a quenching cross section, which describes scattering into any channel other than the incident channel, regardless of what that channel is. The quenching cross section is therefore given by

$$\tilde{\sigma}_{\rm qu} = \tilde{\sigma}_{\rm in} + \tilde{\sigma}_{\rm re} + \tilde{\sigma}_{\rm abs} = g\frac{\pi}{k^2}(1-|\langle S_{aa}\rangle|^2). \tag{23}$$

The corresponding rate coefficients $\tilde{\beta}$ to the cross sections given above are obtained by replacing $1/k^2$ in Eqs. (22) by $\hbar/\mu k$ where μ is the reduced mass of the colliding molecules.

Hereafter, we adopt the perspective of CN theory: S-matrices will be averaged over many resonances, and the resulting mean values will be used to evaluate cross sections.

E. Threshold Behavior

To facilitate applying the CN model to ultracold molecular scattering, it is useful to separate the effects of averaging and absorption from threshold effects due to low collision energies.

Elements of the scattering matrix S_{ij} quantify the amount of incoming flux in channel j that leads to outgoing flux in channel i, where $i, j = a$, b, c, $\ldots$, k, l, m, $\ldots$, ρ, σ, τ $\ldots$. At asymptotic separations r between the collision partners, the wave function is given by

$$\lim_{r\to\infty}\Psi = \psi_j^-(r) - \sum_i S_{ij}\,\psi_i^+(r), \tag{24}$$

in terms of energy-normalized asymptotic incoming and outgoing spherical waves

$$\psi_i^{\pm}(r) = \frac{1}{\sqrt{k_i}}\exp(\pm{\rm i}(k_i r - \pi l_i/2)), \tag{25}$$

where k_i is the asymptotic wave vector for channel i. The S-matrix defined in Eq. (24) is, in general, energy dependent which leads to the usual Bethe-Wigner threshold laws for the cross section [33, 34]. This energy dependence is unrelated to the microscopic interactions between the colliding molecules at small r that dictate the molecular scattering processes. As such these processes are better parametrized by energy-independent short-range quantities. To do so, we employ the ideas and methods of Multichannel Quantum Defect Theory (MQDT) [35–47], which has been successfully applied in various ways and with various notations to the problem of ultracold scattering. At present, the version of this theory most commonly applied in ultracold collisions is the Mies-Julienne version, whose notation we follow here [39, 40].

Scattering theory is usefully described in terms of real-valued, asymptotic reference functions in each channel. These functions are solutions to a single-channel Schrödinger equation, with some predetermined potential. They therefore do not represent free plane waves, but

possesses a phase shift ξ_i, their asymptotic form is

$$f_i(r) = \frac{1}{\sqrt{k_i}} \sin(k_i r - \pi l_i/2 + \xi_i)$$
$$g_i(r) = \frac{1}{\sqrt{k_i}} \cos(k_i r - \pi l_i/2 + \xi_i). \quad (26)$$

In terms of these functions, the asymptotic wave function can be written

$$\lim_{r\to\infty} \Psi = f_j + \sum_i R_{ij}\, g_i, \quad (27)$$

where R_{ij} are the elements of the reactance matrix $\boldsymbol{R}$. The scattering matrix in Eq. (24) is then given by

$$S_{ij} = e^{\mathrm{i}\xi_i} \left(\frac{1+\mathrm{i}\boldsymbol{R}}{1-\mathrm{i}\boldsymbol{R}}\right)_{ij} e^{\mathrm{i}\xi_j} \quad (28)$$

for general running indexes i, j. Defined in this way, the scattering matrix still has an energy dependence due to threshold effects. MQDT gets around this by choosing a new set of reference functions, $\hat{f}_i$, $\hat{g}_i$, defined by WKB-like boundary conditions at short range, in the classically allowed region of channel i (details of these wave functions are given in Ref. 39). For our purposes here the key property of these reference functions is that they are related in a standardized way to the usual energy-normalized asymptotic reference functions by the transformation

$$\begin{pmatrix} f_i \\ g_i \end{pmatrix} = \begin{pmatrix} C_i^{-1} & 0 \\ C_i \tan\lambda_i & C_i \end{pmatrix} \begin{pmatrix} \hat{f}_i \\ \hat{g}_i \end{pmatrix} \quad (29)$$

where $C_i(E)$ and $\tan\lambda_i(E)$ are explicitly energy-dependent factors, with E being the total energy of the system. The dependence of C_i and $\tan\lambda_i$ with energy has been given explicitly near threshold [48], enabling analytical scattering formulas to be constructed.

The pair of reference functions $\hat{f}_i$ and $\hat{g}_i$ are used as follows. Supposing that strong channel couplings lead to a complicated many-channel scattering wave function, nevertheless there is an intermolecular distance r_0 beyond which the channels are essentially uncoupled (this radius is indicated schematically in Fig. 1). The wave function at radii $r > r_0$ can then be written

$$\Psi(r > r_0) = \hat{f}_j + \sum_i Y_{ij}\, \hat{g}_i, \quad (30)$$

in terms of a short-range reactance matrix $\boldsymbol{Y}$. Because of the carefully chosen normalization of $\hat{f}_i$ and $\hat{g}_i$, $\boldsymbol{Y}$ does not carry the energy dependence characteristic of the threshold behavior. From the standpoint of the threshold, $\boldsymbol{Y}$ can be considered constant (later, we will incorporate an explicit energy dependence due to resonant states). The threshold energy dependence is then restored via the transformation

$$\boldsymbol{R} = \boldsymbol{C}^{-1}\left[\boldsymbol{Y}^{-1} - \tan\boldsymbol{\lambda}\right]^{-1}\boldsymbol{C}^{-1}, \quad (31)$$

where $\boldsymbol{C}$ and $\tan\boldsymbol{\lambda}$ are the appropriate diagonal matrices defined in [39]. Alternatively, the energy-independent reference functions can be written in terms of incoming and outgoing waves

$$\hat{f}_i^{\pm} = \hat{g}_i \pm \mathrm{i}\hat{f}_i. \quad (32)$$

The scattering wave function can then be represented at short-range by a scattering matrix $\bar{\boldsymbol{S}}$, defined via

$$\bar{\boldsymbol{S}} = \frac{1+\mathrm{i}\boldsymbol{Y}}{1-\mathrm{i}\boldsymbol{Y}} \quad (33)$$

with inverse transformation

$$\boldsymbol{Y} = \mathrm{i}\frac{1-\bar{\boldsymbol{S}}}{1+\bar{\boldsymbol{S}}}. \quad (34)$$

The bar notation refers to the S-matrix at short-range. In the next section we will apply the statistical theory approach to highly resonant scattering from nuclear physics to replace $\bar{\boldsymbol{S}}$ with a suitably energy averaged version, $\langle\bar{\boldsymbol{S}}\rangle$, that is itself energy independent and includes the absorption effect due to the unobserved and indirect absorption processes.

F. The short-range S-matrix accounting for absorption processes

This section details the construction of the short-range energy-averaged scattering matrix $\bar{\boldsymbol{S}}^{\mathrm{abs}}$, which accounts for any absorption processes that may be present in a given experiment. The elements $\bar{S}_{ij}^{\mathrm{abs}}$ of this matrix are indexed by the observable channels i, $j = a$, b, c, ..., k, l, m, ... It is constructed so that it may be sub-unitary to account for absorption due to the two effects described above, direct absorption and complex formation.

The derivation of this matrix proceeds in three steps: the first constructs an effective, sub-unitary S-matrix $\bar{\boldsymbol{S}}^{\mathrm{unobs}}$ that accounts phenomenologically for direct absorption to unobserved channels, based on an optical potential; the second constructs an energy smooth S-matrix that accounts for absorption due to complex formation by averaging a highly resonant S-matrix $\bar{\boldsymbol{S}}^{\mathrm{res}}$; finally, both types of absorption are combined to obtain a matrix $\bar{\boldsymbol{S}}^{\mathrm{abs}}$ for the combined absorption processes. $\bar{\boldsymbol{S}}^{\mathrm{abs}}$ will then be used in the next section to complete the construction of the matrix $\langle\bar{\boldsymbol{S}}\rangle$.

1. *Absorption due to unobserved channels*

Flux entering in any channel that vanishes due to unobserved processes is conveniently modeled by incorporating a complex-valued optical potential in each channel

$$V_i(r) + \frac{\hbar^2 l_i(l_i+1)}{2m_r r^2} - \mathrm{i}\frac{\gamma_i(r)}{2}, \quad (35)$$

where V_i is the real-valued potential in the absence of such absorption for channel i [15, 49, 50]. In the absence of an exact treatment of the short-range interactions using a full potential energy surface and a full collisional formalism, the influence of the optical potential γ_i is to create a new linear combination of asymptotic functions. Specifically, the short-range Y-matrix in Eq. (30) can be replaced in each channel by a purely imaginary quantity $\mathrm{i}y_i$ [50]. The wave function in this channel now reads

$$\hat{f}_i + \mathrm{i}y_i\,\hat{g}_i, \tag{36}$$

for a real-valued parameter y_i, which we term the *unobserved absorption coefficient* in channel i. The optical potential reproduces the overall phenomenological loss from channel a to all the unobserved channels ρ, σ, τ, ... Recasting the wave function in terms of incoming and outgoing waves from Eq. (32) gives

$$\begin{aligned}\hat{f}_i + \mathrm{i}y_i\,\hat{g}_i =& \frac{1}{2\mathrm{i}}(\hat{f}_i^+ + \hat{f}_i^-) + \frac{\mathrm{i}y_i}{2}(\hat{f}_i^+ - \hat{f}_i^-) \\ =& \frac{\mathrm{i}}{2}(1+y_i)\left[\hat{f}_i^- - \left(\frac{1-y_i}{1+y_i}\right) f_i^+\right].\end{aligned} \tag{37}$$

Here the prefactor $\frac{\mathrm{i}}{2}(1+y_i)$ represents an overall normalization, such that the coefficient of the outgoing wave term in the square brackets gives the short-range scattering matrix

$$\bar{S}_{ii}^{\mathrm{unobs}} = \left(\frac{1-y_i}{1+y_i}\right). \tag{38}$$

This is a unique, overall term for the channel i as the unobserved channels ρ, σ, τ ... are not explicitly enumerated in Eq. (35). We note that $\bar{\boldsymbol{S}}^{\mathrm{unobs}}$ is by definition independent of energy and as such does not need to be energy-averaged.

The coefficients y_i are purely phenomenological parameters of the theory. By considering $0 \le y_i \le 1$, as Ref. 15 does, $\bar{\boldsymbol{S}}^{\mathrm{unobs}}$ is in general sub-unitary, becoming unitary when $y_i = 1$. A special case of this result is in the incident channel, where $i = a$. In this case, $|\bar{S}_{aa}^{\mathrm{unobs}}|^2$ is the probability that the molecules incident in channel a are not lost to the unobserved process. Then, the (short-range) unobserved absorption probability is given by

$$\bar{p}_{\mathrm{unobs}} = 1 - \left(\frac{1-y_a}{1+y_a}\right)^2 = \frac{4y_a}{(1+y_a)^2}. \tag{39}$$

2. *Absorption due to complex formation*

The next step is to include the possibility for the scattering wave function to span the region of the resonances, resulting in indirect absorption due to resonant complex formation. The indirect processes all couple to the dense forest of resonant states μ which results in a highly resonant short-range scattering matrix, here denoted $\bar{\boldsymbol{S}}^{\mathrm{res}}$. As described in Sec. II C, we average the resonant matrix to get an energy-smooth scattering matrix $\langle\bar{\boldsymbol{S}}^{\mathrm{res}}\rangle$.

In order to determine the average of $\bar{\boldsymbol{S}}^{\mathrm{res}}$ we exploit the chaotic nature of highly resonant collisions [51–55], and treat $\bar{\boldsymbol{S}}^{\mathrm{res}}$ statistically using random-matrix theory (RMT) [56, 57]. Here we only sketch the essential steps of the derivation, see Ref. [32] and references therein for a more complete treatment. We first introduce an effective Hamiltonian H^{eff} for the resonances,

$$H_{\mu\nu}^{\mathrm{eff}} = E_\mu\delta_{\mu\nu} - \mathrm{i}\pi\sum_i W_{\mu i}W_{i\nu} \tag{40}$$

in the diagonal representation, which describes the dynamics of the resonances [32, 58]. Eq. (40) is based on a partitioning of the Hilbert space into a bound state space and a scattering channel space, introduced by Feshbach [25–27]. While Eq. (40) is complete, the effort involved in computing all the parameters, especially for the large number of bound states that we are interested in here, make this approach impractical [26]. Following RMT, we therefore consider the parameters as purely statistical quantities. Generally in statistical theories, the energies E_μ of the resonances are assumed to form a distribution whose nearest-neighbor spacing statistics satisfy the Wigner–Dyson distribution with mean level spacing d, and the coupling matrix elements $W_{i\mu}$ between a channel i and a resonant state μ are assumed to be Gaussian random variables with vanishing mean and second moment

$$\langle W_{\mu i}W_{\nu j}\rangle = \delta_{\mu\nu}\delta_{ij}\,\nu_i^2. \tag{41}$$

ν_i is the magnitude of the bound state-scattering channel coupling for channel i. We will, however, not need to specify the distributions for our present purposes.

In terms of the MQDT reference functions $\hat{f}_i$, $\hat{g}_i$ defined above, resonant scattering will result in a short-range $\boldsymbol{Y}^{\mathrm{res}}$ matrix, defined as

$$\Psi = \hat{f}_j + \sum_i Y_{ij}^{\mathrm{res}}\,\hat{g}_i, \tag{42}$$

similar to Eq. (30) with the running indices $i, j = a$, b, c, ..., k, l, m, ... It is assumed that all the resonant states have outer turning points at distances $r < r_0$, so that $\boldsymbol{Y}^{\mathrm{res}}$ contains the full structure of the resonances and therefore takes the form [32]

$$Y_{ij}^{\mathrm{res}} = \pi\sum_\mu \frac{W_{i\mu}W_{\mu j}}{E - E_\mu}. \tag{43}$$

In the weak-coupling limit, $\nu_i \ll d$ the resonances are isolated and can, if desired, be described in terms of resonant widths given by $\gamma_\mu = 2\pi\sum_i |W_{i\mu}|^2$.

In order to average over many resonances, we use the statistical independence of the coupling matrix elements,

$$\langle W_{i\mu}W_{\mu a}\rangle = \delta_{ia}\nu_i^2, \tag{44}$$

to assert that $\langle\boldsymbol{Y}^{\mathrm{res}}\rangle$ is diagonal. This implies that $\langle\bar{S}_{ij}^{\mathrm{res}}\rangle = 0$ if $i \neq j$ which confirms that $\boldsymbol{Y}^{\mathrm{res}}$ contains

no direct contribution to the scattering and describes purely resonant scattering as desired. Moreover, the average of $\boldsymbol{Y}^{\rm res}$ over many isolated resonances is equivalent to the average over a single representative resonance. As the resonances are separated on average by a spacing energy d, this average becomes

$$\langle Y_{ii}^{\rm res}\rangle = \frac{1}{d}\int_{E_\mu-d/2}^{E_\mu+d/2} dE\,\frac{\pi\nu_i^2}{E-E_\mu}. \tag{45}$$

Evaluating this integral in the principal value sense gives

$$\begin{aligned}\langle Y_{ii}^{\rm res}\rangle &\approx \frac{\pi\nu_i^2}{d}\lim_{t\to 0^+}\mathcal{P}\int_{-\infty}^{\infty} dE\,\frac{\exp(\mathrm{i}tE)}{E}\\ &= \mathrm{i}\frac{\pi^2\nu_i^2}{d},\end{aligned} \tag{46}$$

where the contour is closed on the upper half of the complex plane. Therefore, in each channel, the wave function accounting for indirect absorption due to complex formation is given by

$$\hat{f}_i + \mathrm{i}x_i\,\hat{g}_i, \tag{47}$$

in terms of a real-valued parameter

$$x_i = \frac{\pi^2\nu_i^2}{d}, \tag{48}$$

which we term the *indirect absorption coefficient* in channel i. Although coming from an entirely different mechanism, the form of the wave function in Eq. (47) is exactly the same as that for unobserved absorption given by Eq. (36). Similarly, this leads to a short-range scattering matrix in each channel i that corresponds to indirect absorption

$$\langle \bar{S}_{ii}^{\rm res}\rangle = \left(\frac{1-x_i}{1+x_i}\right). \tag{49}$$

This is a unique term for the channel i due to the fact that the off-diagonal elements are zero. Again specializing to the case of the incident channel, $i=a$, the (short-range) indirect absorption probability in channel a is given by

$$\bar{p}_{\rm res} = 1-\left(\frac{1-x_a}{1+x_a}\right)^2 = \frac{4x_a}{(1+x_a)^2}. \tag{50}$$

The unobserved and indirect absorption cases are formally similar. In both cases, the short-range scattering matrix is given by an absorption coefficient y_i and x_i in each channel i. For unobserved processes, the absorption coefficient y_i is a purely phenomenological fitting parameter, whereas for indirect processes, the indirect absorption coefficient x_i contains information about the complex itself, namely, the ratio of bound states-scattering channel coupling to the mean level spacing. The form of x_i is reminiscent of Fermi's golden rule as it connects the average scattering matrix to the square of the bound-continuum matrix element ν_i^2 and the density of states $\rho = 1/d$. It should be noted that this result is quite general, and need not rely on the assumption of weak coupling. Eq. (48) can be derived in a number of ways: using a Born expansion of the S-matrix [32, 59]; via the replica trick [60]; or using the supersymmetry approach [61, 62].

3. *Total absorption*

As the unobserved and indirect cases are formally similar, we can combine both processes to recover the total absorption process in Eq. (22). The resulting short-range scattering matrix is given by

$$\bar{\boldsymbol{S}}^{\rm abs} = \bar{\boldsymbol{S}}^{\rm unobs}\,\langle\bar{\boldsymbol{S}}^{\rm res}\rangle \tag{51}$$

so that

$$\bar{\boldsymbol{S}}_{ii}^{\rm abs} = \left(\frac{1-y_i}{1+y_i}\right)\left(\frac{1-x_i}{1+x_i}\right). \tag{52}$$

The two kinds of effects can be consolidated into a unified form

$$\bar{\boldsymbol{S}}_{ii}^{\rm abs} = \left(\frac{1-z_i}{1+z_i}\right) \tag{53}$$

in terms of an effective *absorption coefficient*

$$z_i = \frac{x_i+y_i}{1+x_iy_i} \tag{54}$$

that combines both unobserved and indirect types of absorption. Fig. 2 illustrates Eq. (54) and the interplay of the different values x_i and y_i. Notice that if either y_i or x_i should be zero, then z_i automatically reverts to the other one.

Once again, specializing to the case of the incident channel $i=a$, The (short-range) absorption probability in the incident channel a as defined in Eq. (5) is then given by

$$\bar{p}_{\rm abs} = 1-\left(\frac{1-z_a}{1+z_a}\right)^2 = \frac{4z_a}{(1+z_a)^2}. \tag{55}$$

Therefore, even in the presence of both types of absorption, if the only observable fact is that absorption has occurred, then a value z_a (or an equivalent parametrisation) can be extracted, as has been done in several studies [11, 15, 18, 63–66].

Finally, the coefficients z, y or x can also depend implicitly on different experimental tools of control such as an electric field $\mathcal{E}$ [10], a magnetic field B, or the intensity of surrounding electromagnetic waves, whether it is due to the surrounding trapping laser [13], red-detuned photo-association [67], or blue-detuned shielding [68–70]. Therefore, the coefficients should carry such dependence so that $z = z(\mathcal{E}, B, I)$, similarly for x and y. We omit this dependence to simplify the notations in the following, unless stated otherwise.

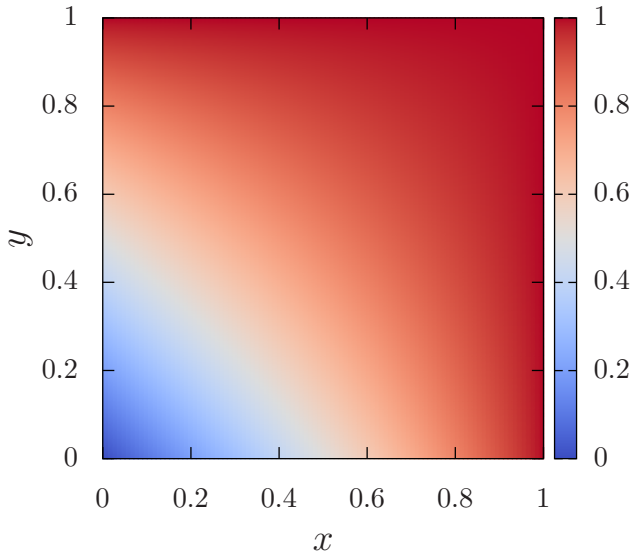

FIG. 2. Interplay of the indirect and unobserved absorption coefficients x and y on the absorption coefficient z given by Eq. (54).

G. The complete short-range S-matrix

We now combine the short-range absorption scattering matrix $\bar{\boldsymbol{S}}^{\rm abs}$, which gathers the unobserved direct processes and all the indirect processes, with a short-range direct scattering matrix $\bar{\boldsymbol{S}}^0$ that includes all the direct processes (elastic, inelastic, reactive) to obtain $\langle\bar{\boldsymbol{S}}\rangle$—which is the energy average of the physical short-range S-matrix of the system of interest $\bar{\boldsymbol{S}}$.

The starting point is a short-range unitary scattering matrix $\bar{\boldsymbol{S}}^0$ that contains all the direct processes such as the molecular elastic, inelastic and reactive scattering in the absence of any absorption due to unobserved channels or complex formation. For example $\bar{\boldsymbol{S}}^0$ could be obtained from a scattering calculation containing only asymptotically open channels. As $\bar{\boldsymbol{S}}^0$ contains no resonances it is by definition energy insensitive and there is no need to take its energy average. $\bar{\boldsymbol{S}}^0$ is defined at r_0 by a wave function of the form

$$\hat{f}_j^- - \sum_i \bar{S}^0_{ij}\,\hat{f}_i^+ \tag{56}$$

restricting, as usual, the indices i, j to the observed channels $i, j = a,\ b,\ c,\ \ldots,\ k,\ l,\ m,\ \ldots$ Starting with this foundation, we transform $\bar{\boldsymbol{S}}^0$ to include the effect of the absorption processes contained in $\bar{\boldsymbol{S}}^{\rm abs}$.

Generically, a short-range process, 1, makes itself apparent through the linear combination of outgoing waves that accompany a certain flux of incoming waves, thus process 1 defines the long-range wave function at $r > r_0$,

$$\boldsymbol{\Psi_1} = \boldsymbol{\mathcal{N}}\left[f^- - \boldsymbol{S_1} f^+\right], \tag{57}$$

where f^- and f^+ are diagonal matrices consisting of incoming and outgoing channel wave functions, respectively, and $\boldsymbol{\mathcal{N}}$ is a overall normalization matrix that is not relevant to our purposes here. We are interested in how the linear combination of f^- and f^+ would change if a second short-range process, for example absorption, would be introduced.

To this end, we first diagonalize $\boldsymbol{S}_1$ so as to write it in terms of its eigenphases δ_α,

$$(S_1)_{ij} = \sum_\alpha \langle i|\alpha\rangle \exp(2\mathrm{i}\delta_\alpha)\,\langle\alpha|j\rangle\,. \tag{58}$$

It is then possible to define the square root of this matrix,

$$(S_1^{1/2})_{ij} = \sum_\alpha \langle i|\alpha\rangle \exp(\mathrm{i}\delta_\alpha)\,\langle\alpha|j\rangle\,. \tag{59}$$

The wave function in the presence of process 1 can then be written

$$\boldsymbol{\Psi_1} = \boldsymbol{\mathcal{N}}\boldsymbol{S_1}^{1/2}\left[\boldsymbol{S_1}^{-1/2} f^- - \boldsymbol{S_1}^{1/2} f^+\right], \tag{60}$$

thus effectively defining a new set of incoming and outgoing reference functions $\boldsymbol{S_1}^{-1/2} f^-$ and $\boldsymbol{S_1}^{1/2} f^+$. We now introduce a second short-range scattering process, which changes the boundary condition of the wave function at the asymptotic matching radius r_0. This new scattering wave function, due to both processes, can be written as a linear combination of the new incoming and outgoing waves, defining a second scattering matrix $\boldsymbol{S_2}$ by

$$\boldsymbol{\Psi_{1,2}} = \left[(\boldsymbol{S_1}^{-1/2} f^-) - \boldsymbol{S_2}(\boldsymbol{S_1}^{1/2} f^+)\right], \tag{61}$$

where we have left off another arbitrary normalization. Finally, factoring out $\boldsymbol{S_1}^{-1/2}$ gives

$$\boldsymbol{\Psi_{1,2}} = \boldsymbol{S_1}^{-1/2}\left[f^- - \boldsymbol{S_1}^{1/2}\boldsymbol{S_2}\boldsymbol{S_1}^{1/2} f^+\right]. \tag{62}$$

This identifies the joint scattering matrix for both processes together as

$$\boldsymbol{S_{1,2}} = \boldsymbol{S_1}^{1/2}\boldsymbol{S_2}\boldsymbol{S_1}^{1/2}. \tag{63}$$

Notice that when we shut off process 1 by setting $\boldsymbol{S_1} = I$ we get $\boldsymbol{S_{1,2}} = \boldsymbol{S_2}$, the scattering matrix in the absence of process 1. Consider for example a single-channel, with $S_1 = \exp(2\mathrm{i}\delta_1)$, $S_2 = \exp(2\mathrm{i}\delta_2)$ then Eqn. (63) simply asserts that the phase shifts add. This approach to combine S-matrices can be applied recursively to include other processes as desired.

Using Eq. (63) can combine $\bar{\boldsymbol{S}}^0$ and $\bar{\boldsymbol{S}}^{\rm abs}$

$$\langle\bar{\boldsymbol{S}}\rangle = \left(\bar{\boldsymbol{S}}^0\right)^{1/2}\bar{\boldsymbol{S}}^{\rm abs}\left(\bar{\boldsymbol{S}}^0\right)^{1/2}. \tag{64}$$

Eq. (64) is the main result of the paper and is quite general. Of course from Eq. (51), $\bar{\boldsymbol{S}}^{\rm abs}$ in Eq. (64) can reduce to either $\bar{\boldsymbol{S}}^{\rm unobs}$ or $\langle\bar{\boldsymbol{S}}^{\rm res}\rangle$ if only unobserved or indirect absorption is present. Therefore, the size of the matrix considered in Eq. (64) can be as high as the number of elastic, inelastic and reactive channels that are observed in an experiment being modeled.

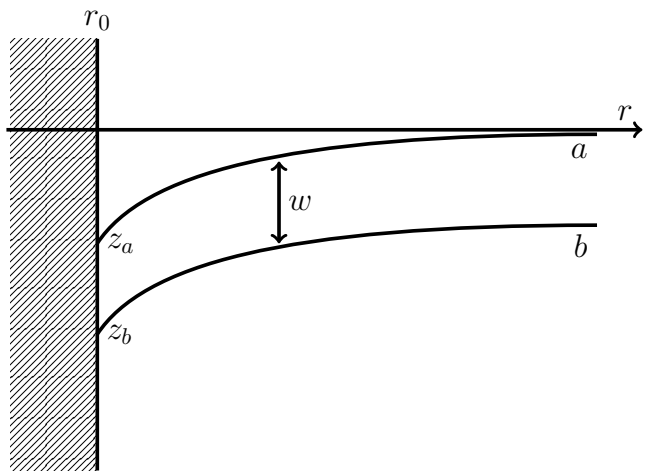

FIG. 3. The two-channel case. The two channels, labelled a and b, are coupled by w. At short-range, absorption from direct and/or indirect processes is described by an effective, absorption coefficient z_a, z_b in each channel.

III. THE TWO-CHANNEL CASE

Rather than study any particular system, in order to gain insight we consider the case with just two open channels, consisting of an incident channel a, and one additional observed channel b, with channel a higher in energy, as illustrated in Fig. 3. We emphasize that while we label the second channel with a b, which identifies the channel with an inelastic scattering process, it could equally well be labelled k, and be identified with a reactive scattering process. Whatever the nature of the scattering to channel b is, we contemplate the scattering process $a \to b$ and the influence that absorption has on this process.

Upon reaching short range $r = r_0$, each channel experiences some kind of absorption with coefficient z_a, z_b, whose exact origin we do not worry about here. It could consist of direct scattering to unobserved channels, or to complex formation, or some combination of both, as described above. In the absence of these processes, the two channels would be somehow coupled and scattering from one to the other could occur when they are both open. Using the convention in [15, 47], we select reference functions $\hat{f}$ and $\hat{g}$ in each channel so that the diagonal matrix elements of the short-range matrix $\boldsymbol{Y}$ vanish [71], as such the scattering length in each channel may appear in the MQDT parameters C and $\tan\lambda$ introduced in Sec. II E. The short-range matrix $\boldsymbol{Y}^0$ is therefore defined by a single, real-valued, off-diagonal coefficient w, via

$$\boldsymbol{Y}^0 = \begin{pmatrix} 0 & \sqrt{w} \\ \sqrt{w} & 0 \end{pmatrix}. \tag{65}$$

This notation uses the letter w to designate the coupling between the observed channels, since y was already used above to denote the unobserved absorption coefficient. This matrix $\boldsymbol{Y}^0$ gives the form of the unitary short-range matrix $\bar{\boldsymbol{S}}^0$ that characterises the direct inelastic/reactive scattering as

$$\bar{\boldsymbol{S}}^0 = \frac{1+\mathrm{i}\boldsymbol{Y}^0}{1-\mathrm{i}\boldsymbol{Y}^0} = \frac{1}{1+w}\begin{pmatrix} 1-w & 2\mathrm{i}\sqrt{w} \\ 2\mathrm{i}\sqrt{w} & 1-w \end{pmatrix} \tag{66}$$

as also given in Ref. [47]. Written in this way, we could of course regard scattering from a to b as yet another absorption process, writing $\bar{S}^0_{aa} = (1-w)/(1+w)$ and identifying an inelastic/reactive absorption coefficient w. However here we are interested in the prospect of observing the molecular product directly, and so to treat the scattering matrix element $\bar{S}^0_{ab}$ explicitly. From Eq. (53), we have

$$\bar{\boldsymbol{S}}^{\mathrm{abs}} = \begin{pmatrix} \frac{1-z_a}{1+z_a} & 0 \\ 0 & \frac{1-z_b}{1+z_b} \end{pmatrix}. \tag{67}$$

To construct the complete short-range matrix $\langle\bar{\boldsymbol{S}}\rangle$ using Eq. (64), we require the square root of $\bar{\boldsymbol{S}}^0$, which is given by

$$\left(\bar{\boldsymbol{S}}^0\right)^{1/2} = \frac{1}{\sqrt{1+w}}\begin{pmatrix} 1 & \mathrm{i}\sqrt{w} \\ \mathrm{i}\sqrt{w} & 1 \end{pmatrix}, \tag{68}$$

from which we obtain

$$\begin{aligned} \langle\bar{\boldsymbol{S}}\rangle &= \left(\bar{\boldsymbol{S}}^0\right)^{1/2}\bar{\boldsymbol{S}}^{\mathrm{abs}}\left(\bar{\boldsymbol{S}}^0\right)^{1/2} \\ &= \frac{1}{1+w}\begin{pmatrix} r_a - w\,r_b & \mathrm{i}\sqrt{w}(r_a+r_b) \\ \mathrm{i}\sqrt{w}(r_a+r_b) & r_b - w\,r_a \end{pmatrix}, \end{aligned} \tag{69}$$

using the shorthand notation $r_i = (1-z_i)/(1+z_i)$, $i = a,b$. The expression in Eq. (69) is quite general. It is however instructive to make the assumption that $z_a = z_b = z$, that is, the two channels experience the same absorption, to simplify results and gain intuition. In this case the short-range matrix $\langle\bar{\boldsymbol{S}}\rangle$ simplifies to

$$\langle\bar{\boldsymbol{S}}\rangle = \frac{1}{(1+w)(1+z)}\begin{pmatrix} (1-w)(1-z) & 2\mathrm{i}\sqrt{w}(1-z) \\ 2\mathrm{i}\sqrt{w}(1-z) & (1-w)(1-z) \end{pmatrix}. \tag{70}$$

Notice that, in a case where channel b were *not* observed, this model would return to the single matrix element $\langle\bar{\boldsymbol{S}}\rangle_{aa} = (1-q)/(1+q)$, written in terms of an effective absorption coefficient

$$q = \frac{w+z}{1+wz} \tag{71}$$

that describes composite absorption from the combination of inelastic/reactive scattering to unobserved channel with absorption due to complex formation. This nicely illustrates the flexibility of the model to treat channels as either observed or unobserved, as required.

To see the basic interplay between direct scattering and absorption, it is worthwhile to consider the probabilities for various outcomes, shorn of the additional complications of threshold effects. Eq. (70) encodes three types of probability:

- the elastic scattering probability for the incident channel a,

$$\bar{p}_{\rm el} = |\langle \bar{S}_{aa} \rangle|^2 = \frac{(1-w)^2(1-z)^2}{(1+w)^2(1+z)^2}. \tag{72}$$

- the probability to enter in channel a and emerge in channel b due to a direct process,

$$\bar{p}_{\rm in} = |\langle \bar{S}_{ba} \rangle|^2 = \frac{4w}{(1+w)^2}\frac{(1-z)^2}{(1+z)^2}. \tag{73}$$

- the absorption probability due to unobserved channels and/or complex formation

$$\begin{aligned} \bar{p}_{\rm abs} &= 1 - |\langle \bar{S}_{aa} \rangle|^2 - |\langle \bar{S}_{ba} \rangle|^2 \\ &= \frac{4z}{(1+z)^2}, \end{aligned} \tag{74}$$

where we recover Eq. (55).

These various probabilities are shown in Fig. 4 as a function of the interchannel coupling w and the absorption coefficient z. As seen in the top figure, the elastic probability is quite low, unless both w or z have a low value. In the other panels the influence of each process on the other can be appreciated. The middle panel shows that direct scattering only happens with appreciable probability when the absorption coefficient z is small, below around 0.2. On the other hand, the absorption probability is indifferent to coupling strength w as can be seen on the bottom panel and implied by Eq. (74) which is independent of w. This kind of absorption is a one-way journey: incident flux that gets to short range is lost and will not emerge from channel b. Note that the coefficients w and z are not interchangeable and do not play equivalent roles in the theory. One observable actually pertains to seeing the scattering end in a particular observable channel, whereas the other is simply absorption.

So far, we have just dealt with the short-range scattering matrix $\langle \bar{\boldsymbol{S}} \rangle$. In order to get the asymptotic S-matrix, $\langle \boldsymbol{S} \rangle$, we need to include threshold effects using MQDT. The QDT parameters C_a and $\tan \lambda_a$ in Eq. (31) are known analytically for s-wave threshold collisions for a $1/r^6$ long-range potential [15, 48]

$$\begin{aligned} C_a^{-2} &\approx k\bar{\rm a}(1 + (s_a - 1)^2), \\ \tan \lambda_a &\approx 1 - s_a, \end{aligned} \tag{75}$$

where $s_a = {\rm a}/\bar{\rm a}$, a being the scattering length in channel a, $\bar{\rm a} = 2\pi R_6/\Gamma(1/4)$ is the Gribakin-Flambaum length [47, 72], $R_6 = (2\mu C_6/\hbar^2)^{1/4}$ is the van der Waals length. We further assume that channel b is far from threshold, as such $C_b = 1$, $\tan \lambda_b = 0$. Following the approach outlined in Section II E, $\langle \boldsymbol{S} \rangle$ and the corresponding cross sections and rate coefficients, can be obtained from $\langle \bar{\boldsymbol{S}} \rangle$ and the QDT parameters in each channel.

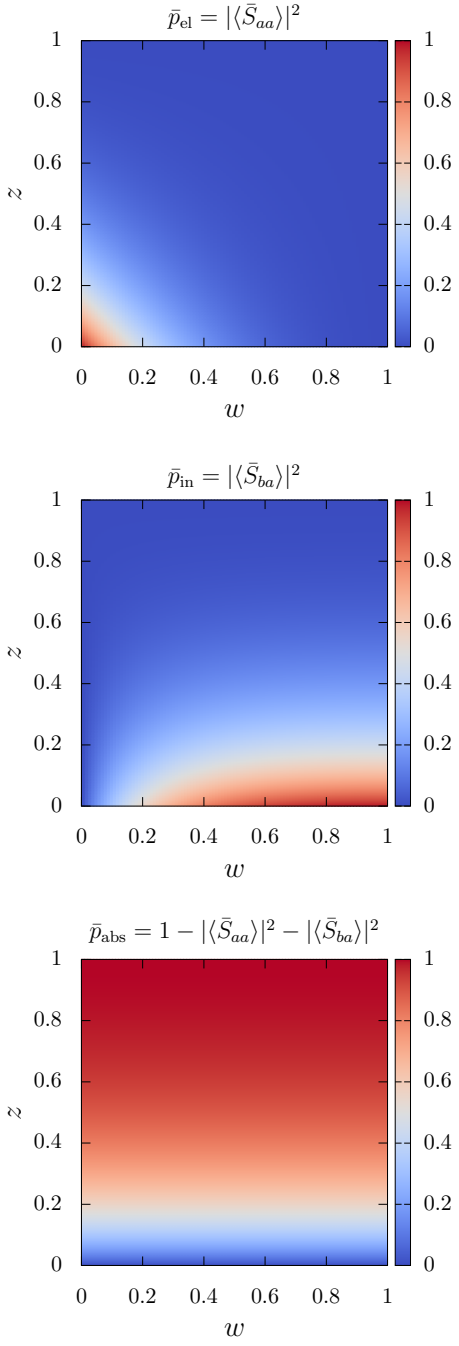

FIG. 4. Top to bottom: short-range probabilities for elastic scattering, inelastic scattering, and absorption, versus the interchannel coupling strength w and absorption coefficient z.

We first consider the case, where no exit channel is explicitly observed. In this case the quenching coefficient q in (71) plays the role of an absorption coefficient. Then q can directly replace y in the quenching formulas of Ref. [47]. For example, the physical quenching probability is

$$p_{\rm qu} \simeq \bar{p}_{\rm qu} \times \frac{C^{-2}(1+q)^2}{(1+q\,C^{-2})^2 + q^2\,\tan^2\lambda}. \tag{76}$$

Here the factor $\bar{p}_{\rm qu} = 4q/(1+q)^2$ is the probability for quenching given that the molecules get close together, while the final factor modifies this probability due to the quantum reflection effects that modify the molecules chances of getting close together. This effect has been discussed at length elsewhere [47] and we do not repeat the discussion here.

In terms of the elastic and quenching rate coefficient, we have from Eq. (26) and Eq. (28) of Ref. [47]

$$\tilde{\beta}_{\rm el} = g\frac{4\pi\hbar}{\mu}k\bar{\rm a}^2\frac{s_a^2+\left(\frac{w+z}{1+wz}\right)^2(2-s_a)^2}{1+\left(\frac{w+z}{1+wz}\right)^2(s_a-1)^2}$$
$$\tilde{\beta}_{\rm qu} = g\frac{4\pi\hbar}{\mu}\bar{\rm a}\left(\frac{w+z}{1+wz}\right)\frac{1+(s_a-1)^2}{1+\left(\frac{w+z}{1+wz}\right)^2(s_a-1)^2}. \quad (77)$$

Of course when $z=0$, two channels with inelastic collisions but no absorption, $\tilde{\beta}_{\rm qu}$ identifies with

$$\tilde{\beta}_{\rm in} = g\frac{4\pi\hbar}{\mu}\bar{\rm a}w\frac{1+(s_a-1)^2}{1+w^2(s_a-1)^2} \quad (78)$$

or when $w=0$, one channel with absorption but no coupling to inelastic channels, $\tilde{\beta}_{\rm qu}$ identifies with

$$\tilde{\beta}_{\rm abs} = g\,\frac{4\pi\hbar}{\mu}\,\bar{\rm a}\,z\,\frac{1+(s_a-1)^2}{1+z^2\,(s_a-1)^2} \quad (79)$$

which are the equations found previously in Ref. [47].

As a simple illustration of the relation between direct scattering and absorption, Fig 5 shows several representative cross sections for the two-channel case. For concreteness, we show cross sections for molecules with the mass and C_6 coefficient of NaRb. In this case, there are several undetermined coefficients, z_a, z_b, s_a, s_b, and w, likely too many to make a meaningful fit to the NaRb data. For this illustration we have somewhat arbitrarily set $z_b = 0.5$, set the incident channel scattering length to $s_a = 1.0$, and set the interchannel coupling to $w = 1.0$, which would give the maximum inelastic scattering in the absence of absorption. Note that the phase parameter s_b in the final channel is irrelevant, as this channel is assumed far from threshold.

The left and right panels in the figure give results for absorption coefficients in the incident channel of $z_a = 0.2$ and $z_a = 0.8$, respectively. In each panel, results from an explicitly two-channel model are shown in color. Specifically, the blue and red curves describe the quenching and inelastic cross sections, respectively. Unsurprisingly, the total quench cross section is greater than the cross section for inelastic scattering alone. As a comparison, the black line shows the cross section that results if we use a one-channel scattering model with the same absorption coefficient $z = z_a$ and phase parameter $s = s_a$ in that channel. It is seen that the inelastic process alters the quenching cross section significantly. The right panel repeats this calculation, for a larger incident channel absorption coefficient $z_a = 0.8$. This larger value of z_a both raises the total quenching cross section, and reduces the relative cross section for inelastic scattering.

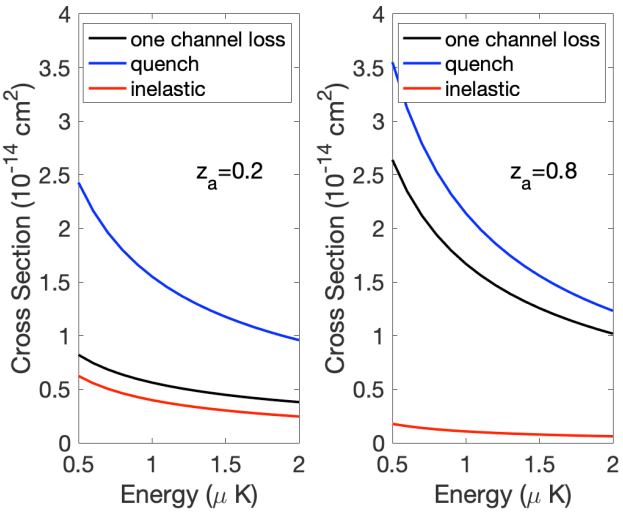

FIG. 5. Schematic cross sections for NaRb molecules colliding in an excited state for two different values of $z_a = 0.2$ (left panel) and 0.8 (right panel). Shown for the two-channel case are the quenching (blue) and inelastic cross sections as computed from Eqs. (72),(73), and (70), fixing $z_a = 0.5$, $s_a = 1.0$, and $w = 1.0$. For comparison, the black curve shows the cross section for the single-channel case ($w = 0$) with an absorption coefficient z_a and phase factor s_a.

In practice, if both the quenching and inelastic cross sections were measured, their energy-dependent cross sections (or temperature-dependent rate coefficients) could be simultaneously fit by formulas such as these, yielding consistent values of the absorption coefficients w, z_a, and z_b, and the incident phase parameter s_a.

IV. APPLICATION TO VARIOUS EXPERIMENTAL SITUATIONS

Cast in terms of the present theory, it is interesting to draw some tentative conclusions about the experiments that have been performed so far. Quantitative description will likely require further information, yet the basic formulas Eq. (55) and Eq. (54) may guide our thinking. Note that in this section we remove the subscript a of the absorption coefficients, for clarity.

A. Collisions of endothermic processes

The most basic collision of ultracold molecules is one in which both molecules are in their absolute ground state and are not chemically reactive and the temperature is low enough such that all other channels are asymptotically closed. This was achieved in collisions of NaRb molecules [9] and RbCs molecules [11]. In this case the presumed losses are due to complex formation, as such z

reduces to x. Light is present in these experiments and may strongly affect the molecular losses [12], therefore x should in general depend on I, the intensity of the trapping laser.

Knowing the energy dependence of the loss cross section enables one to extract the absorption coefficients from experimental data. Thus for NaRb collisions, the fitted parameter gave $x(I) = 0.5$ [18] while for RbCs collisions it gave $x(I) = 0.26(3)$ [11], at the specific laser light intensities of these experiments. While the intensity dependence of x remains unknown, we can make the following assumption. If the light absorption is saturated with intensity, we assume that any complex that is formed decays immediately. In this case the value of x is a measure of the formation of the complex, and represents a direct measure of the ratio between the mean bound state-scattering channel coupling and the mean level spacing of resonances in the complex at the specific laser light intensities. Interpreting the mean coupling as a mean width, via $\nu^2 = \gamma/2\pi$, Eq. (48), would give the ratio of mean resonance width γ to mean level spacing d, $\gamma/d = 2x/\pi$. The ratio would be $\gamma/d = 0.32$ for NaRb and $\gamma/d = 0.17$ for RbCs. Thus the theory produces from the data a concrete prediction that can be used to test a microscopic theory of molecular collisions. This interpretation relies on the assumption that the measured x in the presence of the light truly represents the complex formation. This assumption would of course not be necessary if the measurement were repeated in a box trap.

Even under this assumption, the comparison between empirical and calculated values of γ/d is complicated by the presence of external fields in the experiment, as x can also depend on those fields in addition to the intensity, so that $x = x(\mathcal{E}, B, I)$. For a pure field-free case (no electric field nor magnetic field), a coupled representation scheme can be used to estimate d when the total angular momentum quantum number J and its laboratory projection M are conserved [73]. However, even though the electric field is zero, the NaRb and RbCs measurements are performed in a non-zero magnetic field. It seems therefore appropriate to include in the microscopic estimates, collections of states with different values of J that are mixed by the field. It remains uncertain, however, how many values of J are relevant to the estimate of γ/d for a given magnetic field value. It should also be noted that the application of an electric field appears to alter the absorption coefficient, raising it to the universal value $x(\mathcal{E} > 0) = 1$ [10], indicating that the electric field increases the strength of channel coupling, the density of resonant states, or perhaps both.

B. Chemically Reactive Collisions

An alternative set of experiments, spanning the past decade, has measured loss in ultracold KRb molecules, distinguished from NaRb or RbCs in that the KRb + KRb $\rightarrow K_2 + Rb_2$ reaction is exothermic. In the pioneering experiments [4], the products were not observed, therefore reactive scattering contributed to the unobserved processes described by the coefficient y in addition to the x in the endothermic case. In general, these experiments exhibit loss consistent with an absorption coefficient $z(I) = 1$ from Eq. (54), corresponding to loss of all molecules that get close enough to react or form a collision complex [17]. However, Eq. (54) does not lead to the identification of the separate mechanism for unobserved (chemical reaction in that case) and indirect (complex formation) processes. Nevertheless, the existence of both processes has been verified experimentally, by the identification in REMPI spectroscopy of both the products K_2 and Rb_2, and the intermediaries $K_2Rb_2^+$ [6]. From Eq. (54), we note that in this parametrization $z(I) = 1$ can occur only if $x(I) = 1$ or $y(I) = 1$. It seems likely that indirect loss from complex formation does not occur with unit probability, that is, $x(I)$ is likely less than unity, since this is certainly the case for the non-reactive species NaRb and RbCs (see above). The difference in energies that renders the KRb reaction exothermic, a mere 10 cm^{-1}, is decided at long range as the products recede from one another, and likely has little bearing on the complex itself and the couplings that determine the value of $x(I)$. We therefore provisionally conclude that the loss of KRb molecules with unit probability is mainly due to the unobserved loss (chemical reactions) compared to indirect loss and that $y(I) \simeq z(I) \simeq 1$.

An additional possibility occurs for vibrationally excited states of NaRb [9]. These molecules experience loss due to complex formation when in their ground state, but in their first vibrationally excited state they also have sufficient energy to inelastically de-excite or to chemically react. In this experiment, neither the inelastic nor the reactive products are observed. Therefore, inelastic and reactive processes should be regarded as unobserved absorption processes. The total loss is therefore described by the absorption coefficient $z(I)$ of Eq. (54). Here $x(I)$ would characterize the loss due to complex formation, which, in the simplest interpretation, can be taken as the same as for the non-reactive ground state scattering, $x(I) = 0.5$. While $y(I)$ characterizes the losses due to the inelastic and reactive processes. From the data of the NaRb experiment in $v = 1$, the total absorption coefficient $z(I) = 0.93$ has been extracted [18]. From Eq. (54), we infer that the unobserved absorption coefficient is $y(I) = 0.8$. This value, lying close to unity, emphasizes that the unobserved absorption coefficient, responsible for losses due to inelastic collisions and chemical reactions, takes a high value close to unity, just as in the KRb case.

V. CONCLUSION

As the poet decreed, "Those whom the gods would destroy, they first make mad", and so it is for ultracold molecules. When ultracold molecules collide, a likely outcome is a transformation that releases energy and sends the molecules fleeing from the trap, effectively destroying

the gas. But for ultracold alkali dimers, this destruction need not be immediate, if the molecules first, maddeningly, form a collision complex. Various fates await the molecules upon collisions: elastic scattering, inelastic scattering, reactive scattering, or resonant complex formation. In the work we have detailed a simple quantum-defect model capable of treating all these myriad processes on an equal footing.

In the absence of full scattering matrices, the model captures the essence of these various processes, providing parameterizations of the various cross sections. The model is flexible enough to account explicitly for those processes that are ultimately observed, and to account implicitly for those that are not. The result is a framework capable of being adapted to fit the available data for a given experiment, relating the observables to a small set of parameters. These parameters, in turn, represent a tangible goal for microscopic theories of the four-body dynamics.

The theory as presented treats only the first step of the scattering process, molecules colliding and heading off on one of the paths, elastic, inelastic, reactive, or complex formation. In particular, the theory does not treat the possible decay of the complex, to do so will require a more detailed treatment of the decay rate and product distribution of the complex, work that is currently in progress.

ACKNOWLEDGMENTS

J. F. E. C. acknowledges that this work was supported by the Marsden Fund of New Zealand (Contract No. UOO1923) and gratefully acknowledges support from the Dodd-Walls Centre for Photonic and Quantum Technologies. J. L. B. acknowledges that this material is based upon work supported by the National Science Foundation under Grant Number 1734006, and under grant number 1806971. G. Q. acknowledges funding from the FEW2MANY-SHIELD Project No. ANR-17-CE30-0015 from Agence Nationale de la Recherche.

[1] Wolf, J. *et al.* State-to-state chemistry for three-body recombination in an ultracold rubidium gas. *Science* **358**, 921–924 (2017).

[2] Klein, A. *et al.* Directly probing anisotropy in atom-molecule collisions through quantum scattering resonances. *Nat. Phys.* **13**, 35–38 (2017).

[3] Yang, H. *et al.* Observation of magnetically tunable feshbach resonances in ultracold $^{23}Na^{40}K + {}^{40}K$ collisions. *Science* **363**, 261–264 (2019).

[4] Ospelkaus, S. *et al.* Quantum-state controlled chemical reactions of ultracold potassium-rubidium molecules. *Science* **327**, 853–857 (2010).

[5] Kilaj, A. *et al.* Observation of different reactivities of para-and ortho-water towards cold diazenylium ions. *Nat. Commun.* **9**, 2096 (2018).

[6] Hu, M.-G. *et al.* Direct observation of bimolecular reactions of ultracold KRb molecules. *Science* **366**, 1111–1115 (2019).

[7] Mayle, M., Ruzic, B. P. & Bohn, J. L. Statistical aspects of ultracold resonant scattering. *Phys. Rev. A* **85**, 062712 (2012).

[8] Mayle, M., Quéméner, G., Ruzic, B. P. & Bohn, J. L. Scattering of ultracold molecules in the highly resonant regime. *Phys. Rev. A* **87**, 012709 (2013).

[9] Ye, X., Guo, M., González-Martínez, M. L., Quéméner, G. & Wang, D. Collisions of ultracold $^{23}Na^{87}Rb$ molecules with controlled chemical reactivities. *Science Advances* **4** (2018).

[10] Guo, M. *et al.* Dipolar collisions of ultracold ground-state bosonic molecules. *Phys. Rev. X* **8**, 041044 (2018).

[11] Gregory, P. D. *et al.* Sticky collisions of ultracold RbCs molecules. *Nat. Commun.* **10**, 3104 (2019).

[12] Gregory, P. D., Blackmore, J. A., Bromley, S. L. & Cornish, S. L. Loss of ultracold $^{87}Rb^{133}Cs$ molecules via optical excitation of long-lived two-body collision complexes. *Phys. Rev. Lett.* **124**, 163402 (2020).

[13] Christianen, A., Zwierlein, M. W., Groenenboom, G. C. & Karman, T. Photoinduced two-body loss of ultracold molecules. *Phys. Rev. Lett.* **123**, 123402 (2019).

[14] Liu, Y. *et al.* Steering ultracold reactions through long-lived transient intermediates. *ArXiv e-prints* arXiv:2002.05140 (2020).

[15] Idziaszek, Z. & Julienne, P. S. Universal rate constants for reactive collisions of ultracold molecules. *Phys. Rev. Lett.* **104**, 113202 (2010).

[16] Ni, K.-K. *et al.* Dipolar collisions of polar molecules in the quantum regime. *Nature* **464**, 1324 (2010).

[17] De Marco, L. *et al.* A degenerate fermi gas of polar molecules. *Science* **363**, 853 (2019).

[18] Bai, Y.-P., Li, J.-L., Wang, G.-R. & Cong, S.-L. Model for investigating quantum reflection and quantum coherence in ultracold molecular collisions. *Phys. Rev. A* **100**, 012705 (2019).

[19] Gaunt, A. L., Schmidutz, T. F., Gotlibovych, I., Smith, R. P. & Hadzibabic, Z. Bose-Einstein condensation of atoms in a uniform potential. *Phys. Rev. Lett.* **110**, 200406 (2013).

[20] Feshbach, H., Porter, C. E. & Weisskopf, V. F. Model for nuclear reactions with neutrons. *Phys. Rev.* **96**, 448–464 (1954).

[21] Bohr, N. Neutron capture and nuclear constitution. *Nature* 334–348 (1936).

[22] Feshbach, H. & Weisskopf, V. F. A schematic theory of nuclear cross sections. *Phys. Rev.* **76**, 1550–1560 (1949).

[23] Weisskopf, V. F. Compound nucleus and nuclear resonances. *Helvetica Physica Acta* **23**, 187–200 (1950).

[24] Pauli, W., Rosenfeld, L. & Weisskopf, V. *Niels Bohr and the development of physics* (1957).

[25] Feshbach, H. The optical model and its justification. *Annu. Rev. Nucl. Sci.* **8**, 49–104 (1958).

[26] Feshbach, H. Unified theory of nuclear reactions. *Ann. Phys.* **5**, 357–390 (1958).

[27] Feshbach, H. A unified theory of nuclear reactions. II. *Ann. Phys.* **19**, 287–313 (1962).

[28] Eisenbud, L. *The Formal Properties of Nuclear Collisions.* Ph.D. thesis, Princeton University. (1948).

[29] Wigner, E. P. Lower limit for the energy derivative of the scattering phase shift. *Phys. Rev.* **98**, 145–147 (1955).

[30] Smith, F. T. Lifetime matrix in collision theory. *Phys. Rev.* **118**, 349–356 (1960).

[31] Frye, M. D. & Hutson, J. M. Time delays in ultracold atomic and molecular collisions. *Phys. Rev. Research* **1**, 033023 (2019).

[32] Mitchell, G. E., Richter, A. & Weidenmüller, H. A. Random matrices and chaos in nuclear physics: Nuclear reactions. *Rev. Mod. Phys.* **82**, 2845–2901 (2010).

[33] Bethe, H. A. Theory of disintegration of nuclei by neutrons. *Phys. Rev.* **47**, 747–759 (1935).

[34] Wigner, E. P. On the behavior of cross sections near thresholds. *Phys. Rev.* **73**, 1002–1009 (1948).

[35] Seaton, M. J. Quantum defect theory I. general formulation. *Proc. Phys. Soc.* **88**, 801–814 (1966).

[36] Fano, U. Unified treatment of perturbed series, continuous spectra and collisions. *J. Opt. Soc. Am.* **65**, 979–987 (1975).

[37] Greene, C. H., Fano, U. & Strinati, G. General form of the quantum-defect theory. *Phys. Rev. A* **19**, 1485–1509 (1979).

[38] Greene, C. H., Rau, A. R. P. & Fano, U. General form of the quantum-defect theory. II. *Phys. Rev. A* **26**, 2441–2459 (1982).

[39] Mies, F. H. A multichannel quantum defect analysis of diatomic predissociation and inelastic atomic scattering. *J. Chem. Phys.* **80**, 2514–2525 (1984).

[40] Mies, F. H. & Julienne, P. S. A multichannel quantum defect analysis of two-state couplings in diatomic molecules. *J. Chem. Phys.* **80**, 2526–2536 (1984).

[41] Burke, J. P., Greene, C. H. & Bohn, J. L. Multichannel cold collisions: Simple dependences on energy and magnetic field. *Phys. Rev. Lett.* **81**, 3355–3358 (1998).

[42] Gao, B. Quantum-defect theory of atomic collisions and molecular vibration spectra. *Phys. Rev. A* **58**, 4222–4225 (1998).

[43] Mies, F. H. & Raoult, M. Analysis of threshold effects in ultracold atomic collisions. *Phys. Rev. A* **62**, 012708 (2000).

[44] Gao, B. General form of the quantum-defect theory for$-1/r^\alpha$ type of potentials with $\alpha > 2$. *Phys. Rev. A* **78**, 012702 (2008).

[45] Croft, J. F. E., Wallis, A. O. G., Hutson, J. M. & Julienne, P. S. Multichannel quantum defect theory for cold molecular collisions. *Phys. Rev. A* **84**, 043703 (2011).

[46] Ruzic, B. P., Greene, C. H. & Bohn, J. L. Quantum defect theory for high-partial-wave cold collisions. *Phys. Rev. A* **87**, 032706 (2013).

[47] Jachymski, K., Krych, M., Julienne, P. S. & Idziaszek, Z. Quantum-defect model of a reactive collision at finite temperature. *Phys. Rev. A* **90**, 042705 (2014).

[48] Gao, B. Solutions of the schrödinger equation for an attractive $1/r^6$ potential. *Phys. Rev. A* **58**, 1728–1734 (1998).

[49] Bethe, H. A. A continuum theory of the compound nucleus. *Phys. Rev.* **57**, 1125–1144 (1940).

[50] Osséni, R., Dulieu, O. & Raoult, M. Optimization of generalized multichannel quantum defect reference functions for feshbach resonance characterization. *J. Phys. B: At. Mol. Opt. Phys* **42**, 185202 (2009).

[51] Croft, J. F. E. & Bohn, J. L. Long-lived complexes and chaos in ultracold molecular collisions. *Phys. Rev. A* **89**, 012714 (2014).

[52] Frye, M. D., Morita, M., Vaillant, C. L., Green, D. G. & Hutson, J. M. Approach to chaos in ultracold atomic and molecular physics: Statistics of near-threshold bound states for Li+CaH and Li+CaF. *Phys. Rev. A* **93**, 052713 (2016).

[53] Croft, J. F. E. *et al.* Universality and chaoticity in ultracold K+KRb chemical reactions. *Nat. Commun.* **8**, 15897 (2017).

[54] Yang, B. C., Pérez-Ríos, J. & Robicheaux, F. Classical fractals and quantum chaos in ultracold dipolar collisions. *Phys. Rev. Lett.* **118**, 154101 (2017).

[55] Croft, J. F. E., Balakrishnan, N. & Kendrick, B. K. Long-lived complexes and signatures of chaos in ultracold K_2+Rb collisions. *Phys. Rev. A* **96**, 062707 (2017).

[56] Wigner, E. P. Characteristic vectors of bordered matrices with infinite dimensions. *Ann. Math.* **62**, 548–564 (1955). Wigner, E. P. Characteristic vectors of bordered matrices with infinite dimensions II. *Ann. Math.* **65**, 203–207 (1957).

[57] Dyson, F. J. Statistical theory of the energy levels of complex systems. I. *J. Math. Phys.* **3**, 140–156 (1962). Dyson, F. J. Statistical theory of the energy levels of complex systems. II. *J. Math. Phys.* **3**, 157–165 (1962). Dyson, F. J. Statistical theory of the energy levels of complex systems. III. *J. Math. Phys.* **3**, 166–175 (1962).

[58] Peskin, U., Reisler, H. & Miller, W. H. On the relation between unimolecular reaction rates and overlapping resonances. *J. Chem. Phys.* **101**, 9672–9680 (1994).

[59] Agassi, D., Weidenmüller, H. & Mantzouranis, G. The statistical theory of nuclear reactions for strongly overlapping resonances as a theory of transport phenomena. *Physics Reports* **22**, 145 – 179 (1975).

[60] Weidenmüller, H. A. Statistical theory of nuclear reactions and the gaussian orthogonal ensemble. *Annals of Physics* **158**, 120 – 141 (1984).

[61] Efetov, K. Supersymmetry and theory of disordered metals. *Advances in Physics* **32**, 53–127 (1983).

[62] Verbaarschot, J. J. M. & Zirnbauer, M. R. Critique of the replica trick. *J. Phys. A: Math. Gen.* **18**, 1093–1109 (1985).

[63] Kotochigova, S. Dispersion interactions and reactive collisions of ultracold polar molecules. *New J. Phys.* **12**, 073041 (2010).

[64] Idziaszek, Z., Quéméner, G., Bohn, J. L. & Julienne, P. S. Simple quantum model of ultracold polar molecule collisions. *Phys. Rev. A* **82**, 020703 (2010).

[65] Frye, M. D., Julienne, P. S. & Hutson, J. M. Cold atomic and molecular collisions: approaching the universal loss regime. *New J. Phys.* **17**, 045019 (2015).

[66] Li, H., Li, M., Makrides, C., Petrov, A. & Kotochigova, S. Universal scattering of ultracold atoms and molecules in optical potentials. *Atoms* **7** (2019).

[67] Pérez-Ríos, J., Lepers, M. & Dulieu, O. Theory of long-range ultracold atom-molecule photoassociation. *Phys. Rev. Lett.* **115**, 073201 (2015).

[68] Lassablière, L. & Quéméner, G. Controlling the scattering length of ultracold dipolar molecules. *Phys. Rev. Lett.* **121**, 163402 (2018).

[69] Karman, T. & Hutson, J. M. Microwave shielding of ultracold polar molecules. *Phys. Rev. Lett.* **121**, 163401

(2018).
[70] Karman, T. Microwave shielding with far-from-circular polarization. *Phys. Rev. A* **101**, 042702 (2020).
[71] Giusti-Suzor, A. & Fano, U. Alternative parameters of channel interactions. I. symmetry analysis of the two-channel coupling. *J. Phys. B: At. Mol. Opt. Phys* **17**, 215 (1984).
[72] Gribakin, G. F. & Flambaum, V. V. Calculation of the scattering length in atomic collisions using the semiclassical approximation. *Phys. Rev. A* **48**, 546 (1993).
[73] Christianen, A., Karman, T. & Groenenboom, G. C. Quasiclassical method for calculating the density of states of ultracold collision complexes. *Phys. Rev. A* **100**, 032708 (2019).